International Journal of Biological Macromolecules 93 (2016) 20–26

Contents lists available at ScienceDirect

International Journal of Biological Macromolecules

journal homepage: www.elsevier.com/locate/ijbiomac

Engineering increased thermostability in the GH-10 *endo*-1,4-β-xylanase from *Thermoascus aurantiacus* CBMAI 756

Angelica R. de Souza[a], Gabriela C. de Araújo[a], Letícia M. Zanphorlin[c], Roberto Ruller[c], Fernanda C. Franco[a], Fernando A.G. Torres[b], Jeffrey A. Mertens[d], Michael J. Bowman[d], Eleni Gomes[a], Roberto Da Silva[a,*]

[a] *UNESP (São Paulo State University – Júlio de Mesquita Filho), Biochemistry and Applied Microbiology Laboratory, São José do Rio Preto, SP 15054-000, Brazil*
[b] *University of Brasília, Department of Cell Biology – Brasília, Distrito Federal, Brazil*
[c] *CTBE (Brazilian Bioethanol Science and Technology LaboratoryatNational Center for Research in Energy and Materials), Campinas, SP 13083-100, Brazil*
[d] *Bioenergy Research Unit, National Center for Agricultural Utilization Research, USDA – ARS, 1815 N, University St, Peoria, IL 61604, USA*

ARTICLE INFO

Article history:
Received 1 April 2016
Received in revised form 13 July 2016
Accepted 20 August 2016
Available online 21 August 2016

Keywords:
Protein engineering
Rational design
Endo-xylanase
Site-directed mutagenesis
Thermostability

ABSTRACT

The GH10 *endo*-xylanase from *Thermoascus aurantiacus* CBMAI 756 (XynA) is industrially attractive due to its considerable thermostability and high specific activity. Considering the possibility of a further improvement in thermostability, eleven mutants were created in the present study via site-directed mutagenesis using XynA as a template. XynA and its mutants were successfully overexpressed in *Escherichia coli* Rosetta-gami DE3 and purified, exhibiting maximum xylanolytic activity at pH 5 and 65 °C. Three of the eleven mutants, Q158R, H209N, and N257D, demonstrated increased thermostability relative to the wild type at 70 °C and 75 °C.Q158R and N257D were stable in the pH range 5.0–10.0, while WT and H209N were stable from pH 8–10. CD analysis demonstrated that the WT and the three mutant enzymes were expressed in a folded form. H209N was the most thermostable mutant, showing a T*m* of 71.3 °C. Molecular dynamics modeling analyses suggest that the increase in H209N thermostability may beattributed to a higher number of short helices and salt bridges, which displayed a positive charge in the catalytic core, stabilizing its tertiary structure.

1. Introduction

Hemicelluloses are the most abundant heteropolysaccharides in nature,representing about 20–35% of the lignocellulosic biomass [1] depending on the type of plant. Xylan is the main constituent of hemicelluloses and the second most abundant cell wall polysaccharide. It interact with cellulose, lignin and other cell wall components in a way that is relevant to the resistance and cellular integrity [2,3]. It consists of a homopolymeric backbone of β-1,4-xylopyranose residues, including some branch points(α-1,3-arabinose and α-1,2-glucuronicresidues, for instance) [4].Its hydrolysis can be catalyzed by the *endo*-1,4-β-xylanase (E.C. 3.2.1.8) [5], with consequent release of xylooligosaccharide units.

In the last decade, increased attention has been devoted to *endo*-1,4-β-xylanases because of their wide range of industrial applications, either alone or in combination with other hemicellulases [6]. These enzymes have been applied in food and feed processing industries, biobleaching ofkraftpulp [5,7,8] andthe biofuels industry, where they are employed in the conversion of the lignocellulosic biomass into fermentable sugars [7,9,10]. However, severe reaction conditions (e.g. extreme temperatures and pH) restrict the industrial applications of *endo*-xylanases [7,11,12]. As a result,attempts to improve the thermostabilityof several microbial xylanase enzymes (fungal and bacterial) bydirected evolution havebeen reported [12–17]

XynA, the wild-type GH10 *endo*-xylanase from *T. aurantiacus*, is very attractive for biotechnological applications due to its considerablethermostability and high specific activity [18,19]. Site-directed mutagenesis is regarded as a promising strategy for further improvement of enzymes [18] in relation to theirability to withstand high temperatures. In the present study, the gene*XynA*,encoding a GH10 xylanase of *T. aurantiacus*CBMAI 756,was cloned and recombinantly overexpressedin *E. coli* for useas a platform for the construction of site-directed mutants. The mutants were subjected to biochemical and biophysical character-

* Corresponding author.
E-mail addresses: dasilva@ibilce.unesp.br, dasilva_so@yahoo.com.br (R. Da Silva).

http://dx.doi.org/10.1016/j.ijbiomac.2016.08.056
0141-8130/

ization and the three most thermostable constructs were chosen for more in-depth studies. The secondary structure of the mutant proteins was obtained by molecular modeling and the structural features determined by molecular dynamics,showing the effect of the change of amino acid residues on thermostability. These three mutants are good candidates for future molecular approaches using directed evolution, to obtain even more thermostable xylanase enzymes.

2. Material and methods

2.1. Cloning of the XynA gene

The plasmid PIC9XynA was constructed by Franco (2014) [20] from the thermophilic fungus *T. aurantiacus* CBMAI 756, which was obtained from the Biochemistry and Applied Microbiology Laboratory culture collection, IBILCE/UNESP. It was isolated from a decaying hemicellulosic material collected in the state of Amazonas, Brazil [21]. The gene *XynA* without signal peptide (909 bp) was amplified with Q5 High-Fidelity DNA polymerase (New England Biolabs, Beverly, MA) using the primer set pET-28aXynA,with plasmid pPIC9XynA as template (Table 1). The forward and reverse primers added *Nco*I and *Not*I restriction sites, respectively, which allowed the ligation of the ORF into a pET-28a expression vector in-frame with a C-terminal 6XHis-tag. The XynA gene was amplified in 50 μL reactions using 0.2 ng of DNA (pPIC9XynA)as the template, 0.2 mM dNTP's, 0.2 pmol μL^{-1} each primer and 0.02 U μL^{-1} of Q5® High-fidelity polymerase. Cycling conditions were performed following kit instructions: initial denaturation at 98 °C for 10 s:30 cycles at 98 °C for 30 s, 60 °C for 30 s and 72 °C for 30 s; and final extension at 72 °C for 2 min. The amplicon was purified using MinElute PCR Purification kit (Qiagen),digested with Nco1 and Not1and ligated into a pET28a using T4 Ligase (Promega). The resulting pET-28a_XynAconstruct was used to transform chemically competent NEB 10-beta *E. coli* cells (New England BioLabs) and plated on LB-agar supplemented with kanamycin (50 $\mu g\,mL^{-1}$) for selection and propagation. The pET-28a_XynA construct was sequenced to verify the fidelity of the gene.

Table 1
Oligonucleotide pairs used for plasmid construction and site-directed mutagenesis.

Constructions	Oligonucleotide sequences (5′ → 3′)[a]
pET28aXynAsystem[b]	GG*CCATGG*GCCAAGCTGCACAGAGT GG*GCGGCCGC*TCACTGCTGCAGG
R124A	GGCAAGATC**GC**TGCATGGGACGTG CTTGTACCGGGTCATCAAGG
R190A	CATTGTCAAC**GC**CGTCAAGCAA GCCTGCGTCTTGGGGTACGA
Q158R	GATTGCTTTCC**GA**ACCGCCCGCG GGGATGTAATCCTCCCCGATG
Y181K	CAGTGCCTCG**AAA**CCCAAGACGCAG TCGAGGTTGTAATCGTTGAT
L219D	GAGCCAGTGTT**GAT**CAGGCTCTTCCG CCTGACCAGCGCTGAGGTGCG
H209N	GGATCGCAAACG**A**ACCTCAGCGCTG TATGCCGTCAATCGGGACTCC
H83N	CCGTGGC**A**ATACTCTTGTATGG ATCAGCTTTCCATTTTGCTGG
N250D	GATTACGTC**G**ATGTCGTGAACG CGTCGAGCTAGCACCAGCCACG
N257D	CGCTTGCCTC**G**ACGTGCAGTCC TTCACGACATTGACGTAATCCG
Q259D	CTCAACGTG**GA**T**T**CCTGCGTGGG GCAAGCGTTCACGACTTG
C255G	CGTGAACGCT**G**GCCTCAACGTG ACATTGACGTAATCCGTCGAGC

[a] The nucleotide alterations achieved by site-directed mutagenesis are underlined.
[b] Cleavage sites for the restriction enzymes (*Nco*I and *Not*I) are in italics and underlined.

2.2. Site-directed mutagenesis

For all mutations, a rational design was used, based on the three-dimensional structure deposited in PDB (1TUX). C255G was designed to explore the protein expression effect after the change of the unique Cys of the C255-C261 disulfide bond, which is conserved in the majority of the xylanases in family F/10 [22]. The generation of other mutants was proposed to investigate the stability and improve the catalytic power of the xylanase from *T. aurantiacus*. The contribution of the amino acid position on the salt bridge, either buried (R124-Q232) or on the surface (R190-Q150), was investigated for the mutations R124A and R190A. Mutants H209N and H83N were designed to observe whether the His residues are related to the ionization effects of the catalytic Glu residues as reported by Natesh et al. [18]. Mutants L219D, N250D, N257D, Q259D, Q158R and Y181K were constructed to increase the number of acidic and basic amino acid residues in XynA, which could contribute to create more salt bridge interactions [23] in its structure.

Eleven site-directed mutations were constructed using the Q5® Site-Directed Mutagenesis kit (New England Biolabs) following the manufacturer's instructions. Reactions contained 0.5 μM of each oligonucleotide pair (Table 1) and 25 ng of pET-28a_XynA plasmid DNA as template. The annealing temperature was set at 54 °C. The mutant constructs were transformed in NEB 5-alpha chemically competent *E. coli* cells and plated on LB agar supplemented with kanamycin (50 $\mu g\,mL^{-1}$). All mutant constructs were confirmed by DNA sequencing.

2.3. Heterologous expression, enzyme purificationand quantification

The pET-28a_XynA wild type and mutant plasmid constructs were used to transform Rosetta-gami (DE3) cells (Novagen) for heterologous expression. For recombinant and all mutants protein expression, cultures were initially grown at 37 °C and 250 rpm in 50 mL of LB medium supplemented with kanamycin (50 $\mu g\,mL^{-1}$) until reaching an OD_{600} of 0.5. Protein expression was induced by the addition of 0.4 mM isopropyl-β-D-1-thiogalactopyranoside (IPTG) and grown for an additional 4 h at 37 °C and 250 rpm The cells were collected by centrifugation (10 min at 10,000 x *g*) and disrupted using BugBuster® 1× Protein Extraction Reagent (Novagen) in the presence of Lysonase (10 $\mu L\,g^{-1}$ cells). Both soluble and insoluble fractions were analyzed by SDS-PAGE electrophoresis and enzymatic activity, as described below.

The wild-type (WT) and mutant enzymes were purified from the crude cell extract using a HisPrepFF 16/10 column (GE Healthcare Life Sciences) and an Akta Purifier FPLC system (GE Healthcare Life Sciences). Protein samples were concentrated (Amicon 10,000 NMWL concentrators, Merck Millipore) and quantified(Varian Cary 50 Bio UV–vis spectrophotometer, Agilent Technologies) at 280 nm, considering a molar extinction coefficient of 57,660 [24]. All steps of enzyme expression and purification were analyzed by SDS-PAGE electrophoresis using (12%) SDS polyacrylamide gels [25] with Broad Range molecular marker (200–6.5 kDa, Bio-Rad).

2.4. Biochemical, biophysical and structural properties of XynA (WT) and mutants

2.4.1. Effects of temperature and pH on xylanase activity and stability

Unless otherwise stated, the xylanolytic activity was determined by the 3,5-dinitrosalicylic acid (DNS) method [26] in a micro-plate assay, as described [27], in a 5-min reaction, using 1% xylan from beechwood (Sigma) as substrate at 65 °C and pH 5.0. One xylanase unit is defined as the amount of enzyme required to generate 1 μmol of reducing sugar per min, using xylose as a standard product. A control reaction consisted of the addition of the enzyme after reaction incubation with DNS. All assays were performed in triplicate.

The optimal temperatures for enzymatic activity were tested in reactions performed in 50 mM sodium acetate buffer pH 5, over the temperature range from 40 to 80 °C. Thermostability was assessed by incubation of the enzyme for 1 h at 70 °C and 75 °C. The residual activities were calculated as percentages of the initial activity without treatment (100%) [28]. The optimal pH values and pH stability of the enzymes were determined by assays in a wide pH range, using 50 mM of four different buffer solutions (pH 3.0: glycine-HCl; pH 3.5–5: sodium acetate; pH 5.5–9: tris-aminomethane, and pH 9.5–10.5: glycine). Optimal pH was determined at 65 °C, while for the pH stability measurements, the enzymes were first incubated for 24 h without the substrate at room temperature, followed by activity assays at 65 °C in pH 5. The residual activities were compared to a control reaction, without treatment (100%) [28].

2.4.2. Spectroscopic analyses

Circular Dichroism (CD) measurements were carried out in a Jasco-815 spectropolarimeter with a Peltier-type temperature control system. All experiments were analyzed using a protein concentration range of 2–3.5 μM in 20 mM HEPES buffer, 50 mM NaCl, pH 7.4. Thermal unfolding experiments monitored by CD signal were performed with a melting rate of 1 °C/min at 220 nm. All CD profiles were normalized for molar residual ellipticity (MRE) and the temperature at the midpoint transition (T*m*) was obtained by fitting the CD data to a sigmoidal Boltzmann function using the software Origin 8.1.

2.4.3. Molecular modeling and molecular dynamics simulation of XynA and its thermostable mutants in solution

The 3-D structures of XynA and its mutants (Q158R, H209N and N257D) were homology-modeled using the program MODELLER 9.9 [29] based on a known crystal structure of XynA (PDB code: 1TUX). They were subjected to Molecular Dynamics (MD) simulation processes for 50 ns at 338 K in water containing 100 mM NaCl and pH5.0, using the GROMACS molecular dynamics package (version 4.5.5) [30,31]. GROMOS53A6 force field [32] and Single point charge (SPC) as water model [33] were used to construct themodels of XynA and the mutants. The temperature was kept constant using V-rescale [34] thermostat with coupling constant $\tau = 0.1$ ps^{-1}. Constant pressure was held at 1 atm by a Berendsen barostat [35] with coupling constant $\tau = 0.1$ ps^{-1}. Integration of Newton's equation of motion was performed by the leapfrog algorithm with a time step of 2 fs. Long-range electrostatic interaction was treated using fast particle-mesh Ewald electrostatics (PME) [36]. A cutoff of1. 25 nm was implemented for the Lennard–Jones and the direct space part of the Ewald sum for Coulombic interactions. The Fourier space part of the Ewald splitting was computed using the particle-mesh Ewald method [36], with a grid length of 0.15 nm.

Thermostability was monitored by root mean square fluctuation (RMSF), analysis of the secondary structure (Procheck) [37], number of hydrogen bonds (tool g_hbond, GROMACS) and salt bridges (Pymol) [38]. The residual α-carbon flexibility and the number of hydrogen bonds were calculated by the tools g_rmsf and g_hbond from GROMACS, respectively. The evaluation of salt bridge formation was performed using the ESBRI interface [39].

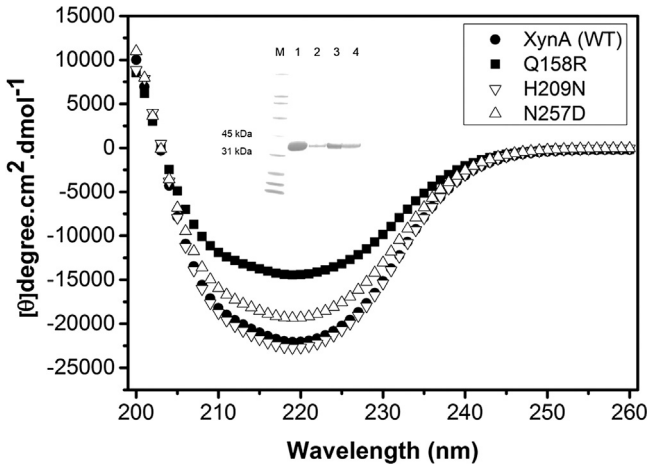

Fig. 1. Secondary structure of XynA and its mutants after purification. MRE of mutants showing that all enzymes had a predominantly α-helix profile with a minimum at 220 nm. (Inset), SDS-PAGE analysis of the *endo*-xylanase variants after the purification and concentration steps. (M) SDS-PAGE molecular weight standard, Broad Range (Bio-Rad) 200; 116.3; 97.4; 66.2; 45; 31; 21.5; 14.4; 6.5 kDa. Line 1 = XynA (30 μg); lines 2, 3 and 4 = H209N (3 μg), Q158R and N257D (5 μg), respectivelly.

3. Results and discussion

3.1. Expression and purification of XynA and the mutants

XynAand its mutants were successfully expressed as soluble proteins in Rosetta-gami (DE3) cells (Table 2), yielding highly purified protein (Fig. 1. Insert) of the expected molecular weight (~33 kDa). This is the first report of successful recombinant overexpression of mutant and WT XynA from *T. aurantiacus* using *E. coli.*

3.2. Biochemical properties of XynA and the mutants

As observed in Table 2,XynA (WT) presented the greatest activity at 65–75 °C and pH 5, while all mutants had the highest activity values at 65 °C and pH 4.5–5.0.The only exceptions were R190A and N257D, which presented slightly different values (70 °C,pH 4.5–5.5).Thus, the following experiments were performed at 65 °C and pH 5, as specific activity values for all the enzymes presented only negligible standard deviations in this assay condition. Based on obtained results from Table 2 the next step was the selection of mutants with increased thermal stability regarding to the native enzyme at 70 °C and 75 °C.

In thermostability assays, the three best mutants, Q158R, H209N, and N257D, presented a significantly higher residual activity than XynA (Table 3), 1.8–2.5 fold higher at 70 °C and 2.6–8 fold at 75 °C, thus confirming the success of the site-directed mutagenesis assays and the great potential for use of these three mutant enzymes in future experiments involving thermostability. All other mutants were less stable than the three selected mutant enzymes (data not shown). In all temperatures, the least activity was observed for N257D and the greatest for H209N. Khandke et al. [22] reported that XynA isolated from *T. aurantiacus* showed full activity after 8 h at 70 °C. However, this level of stability was not observed in our assays when the enzyme was incubated without substrate. It is unclear from the original work whether the native enzyme was incubated in the presence of substrate, which would

Table 2
Total protein content, specific activities in the optimum temperature and ideal pH and temperature for all the enzyme variants constructed in this work.

Enzyme Variants	Total protein (mg 100 mL^{-1})	Specific Activity (U mg^{-1})	Optimum T (°C)	Optimum pH
XynA	3.12	1283.96 ± 39.60	65–75	5
R124A	0.72	855.93 ± 61.71	65	4.5
R190A	6.10	1132.61 ± 19.29	70	4.5
Q158R	0.67	762.74 ± 6.01	65	4.5
Y181K	2.11	1087.41 ± 40.82	65	5
L219D	4.73	1318.53 ± 22.64	65	5
H209N	6.92	1849.03 ± 112.89	65	5
H83N	2.45	17.71 ± 2.41	65	4.5
N250D	0.74	1092.30 ± 108.30	65	5
N257D	3.47	549.88 ± 5.59	70	5.5
Q259D	1.67	922.59 ± 48.22	65	5
C255G	4.82	954.56 ± 45.02	65	5

Table 3
Residual activities of XynA (WT) and the best mutant enzymes at 70 °C and 75 °C and some of their structural features*Tm* values were monitored by the MRE signal at 220 nm. The number of salt bridges and short helices was obtained after 50 ns simulation in water with NaCl (100 mM) at 338 K.

	(70 °C) Residual activity (°)	(75 °C) Residual activity (%)	Tm (°C)	Salt bridges	Short helices
XynA	30.28 ± 2.27	5.94 ± 1.99	70.9	13	1
Q158R	61.52 ± 4.70	28.32 ± 5.14	70.9	15	3
H209N	76.52 ± 0.59	47.46 ± 5.99	71.3	17	4
N257D	53.93± 2.11	15.91 ± 2.55	70.4	15	2

provide a stabilizing effect on the enzyme [40], contributing to an increase in its thermostability. These three mutants were chosen to continue the work.

The pH stability of enzymes is presented in Fig. 2. The residual activity of XynA at optimal pH 5 is about 35% at pH 5 and at pH 4, near 40%, which is not statistically different given the deviation. It increased continuously from pH 5 to pH10 (>90%). So, it presented a good stability in the basic area that was dependent of the increase of pH and, a reduced stability in the acidic zone. These data suggest that the treatment for 24 h in basic pH exhibited a positive effect retaining the activity. In the acidic area, the enzyme worked with about 40% of its stability. Although the optimum pH is around 5, the long incubation time may have caused a destabilizing effect on the tertiary structure, leading to a loss of catalytic activity.

It is difficult to explain the behavior of an enzyme under pH variation due to several factors that influence the protein, such as p*K*a of several of its amino acids, amino acids arrangement in relation to the active site, protein pI and types of attractive interactions.These factors, acting together and coordinately, determine the shape and stability of the tertiary structure of proteins, and consequently, their activity. There are two possible arguments that can explain this behavior of XynA: it is known that enzymatic action can be influenced by pI [41]. The maintenance of the enzyme in acidic condition near the pI for a long time can lead to unfolding of the structure and reducing its activity at optimum pH. The closerto pI is the pH of the enzyme's incubation, the lower the residual activity it presents, leading enzymatic activity to pH dependence. Another point is regarding the deprotonation of key residues that could give rise to several changes which are unfavorable to the native state, including electrostatic repulsions, destruction of salt bridges and the formation of buried isolated charges, eventually leading to functional loss of activity [42]. The possibility of these factors acting together should not be excluded.

Interestingly, Q158R and N257D exhibited higher pH stability profiles than all other mutants, with enzymatic activity remaining constant in the whole pH range investigated (Fig. 2). The mutations Q158R and N257D involve a neutral charge amino acid exchange (Gln and Asn) to a charged amino acid with positive (Arg) and negative (Asp) charges, respectively. These data suggest the mutations on the surface by charged amino acids increased the stability against different pHs.

On the other hand, mutant H209N had a reduced stability compared to the WT, probably because the His residue at position 209 may have an important role on the catalytic site, acting as the ionization effect upon the Glu residues in the catalytic core of the enzyme, such as described by [18]. Therefore, the substitution by an Asn provoked a loss on enzymatic activity (Fig. 1). Also, it is possible the salt bridges did not form correctly [43], especially at acidic pHs. As a result, H209N exhibited a sharp increase from pH 9.0–10.

3.3. Spectroscopic analyses

CD spectra analyses (Fig. 1) revealed that XynA and the mutant constructs were purified in a folded conformation, with a negative minimum at 220 nm, suggesting a predominantly α-helix structure for all the proteins. Interestingly, mutants N257D and Q158R had a smaller CD signal at 220 nm than the other two enzymes, especially in the case of Q158R, which might indicate that the enzyme was

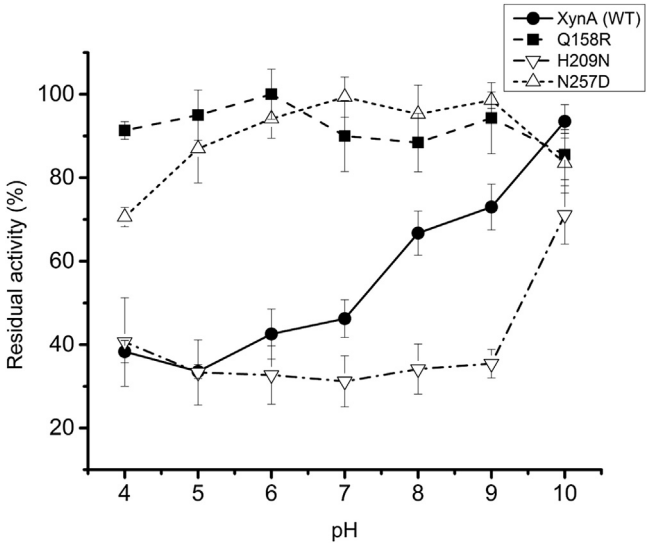

Fig. 2. pH stability profile. -●- XynA; -■- Q158R; -▼- H209N; and -Δ- N257D. A clear preferential activity is observed for H209N and XynA (WT) in the basic zone, whereas Q158R and N257D presented a high residual activity in the whole pH range.

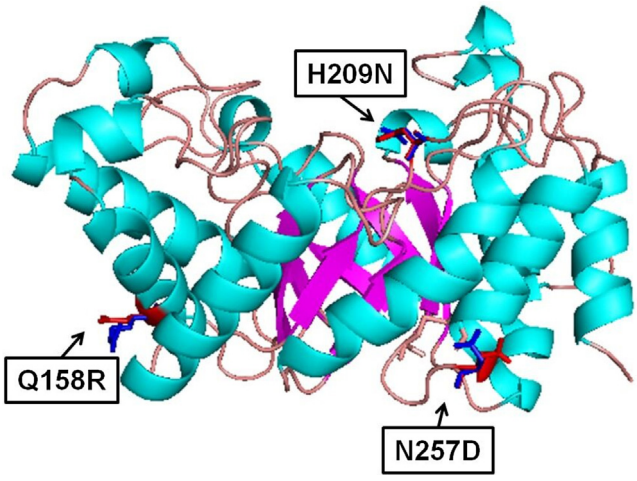

Fig. 3. Model structure of XynA (WT) built by MODELLER based on the PDB ID code 1TUX. Mutants Q158R, N257D and H209N are highlighted. The red sticks are the amino acids from XynA and the blue sticks are the modified amino acids. (For interpretation of the references to color in this figure legend, the reader is referred to the web version of this article.)

losing its folded structure. H209N was the most thermostable of the mutants,making it the most successful mutant constructed in this study in terms of thermostability.

To understand how the mutations (Q158R, H209N and N257D) affectedthe thermostability of the recombinant *endo*-xylanase (GH10 XynA), these purified constructs were heated to 90 °C and monitored by CD signal at 220 nm. MRE (Mean residue ellipticity)data of each construct were obtained as a function of temperature(Table 3), revealing T*m* (melting temperature)values of 70.4–71.3 °C, which confirms them to be thermophilic enzymes. More interestingly, XynA (WT) (T*m*70.9 °C)was observed to be more thermostable than most of the other xylanases described in literature [44]. For instance, the GH11 xylanase from *Thermomyces lanuginosus*has a T*m* of 66 °C [45], while the GH10 xylanase from *Trichoderma reesei* has a T*m* of 62 °C [46]. Furthermore, although the differences among the mutants were small, mutant H209N was slightly more thermostable than XynA and the other constructs, presenting a T*m*of 71.3 °C (Table 3).

3.4. Molecular modeling and molecular dynamics simulation

As observed in the molecular dynamics simulation using GROMACS at 338 K (Fig. 4), the secondary structures of all mutants were very similar to that observed for XynA, conserving the $(\alpha/\beta)_8$ TIM-barrel fold structure. Also, the validation results of the models were performed by SAVES server (Table S1). All models presented atom volumes acceptable for a structure with good and refined resolution, showing a score lower or equal to 5%. They had an ERRAT score equivalent to models with resolution of the order 2.5–3 Å and presented more than 99% identity with amino acids with a score equal to or higher than 2.0, which indicating good quality models.

RMSF is a measure of the displacement of a particular atom, or group of atoms, relative to the reference structure. In this study, flexible residues were defined as the residues showing the highest α-carbon flexibility among all the residues in a protein, thus presenting higher RMSF values. Rigid residues were defined as the residues showing the lowest flexibility (lower RMSF values). RMSF results showed the mutants have some high fluctuations in the N-terminal and C-terminal regions, more specifically between β2-β3 and between β3-β4. However, mutants Q158R, H209N and N257D did not change the RMSF profile in these positions nor the fluctuation of the eight sheets that compose the protein core (Fig. S2). Studies suggest that the protein core is the main determinant of protein stability and activity [47,48]. For instance, even though the mutation in H209Nis close to the protein core (Fig. 3), the stability of core was conserved, therefore xylanase activity was maintained.

Natesh et al. [18] showed that the substrate-binding site of four xylanase structures from family F/10 occurred in negatively-charged regions. However, XynA and the mutants presented positive and negative charges in the surface of the substrate-binding site (Fig. S3), with more positive charges in H209N than in the other models. As the highest specific activity (~1850 U mg^{-1}) was observed in this mutant, these data may suggest an influence of the charges in the substrate-binding site on xylanolytic activity, with specific activity increased for the model with more positive charges at the binding site. In this sense, XynA (1290 U mg^{-1}) and Q158R (765 U mg^{-1}) exhibited a similar distribution of charges with buried negative charges, while N257D, which presented the lowest specific activity measured (550 U mg^{-1}), displayed negative charges more exposed to the surface than the other enzymes. This suggests a relationship between charge potential in the active site and specific activity. Further work is required to confirm this relationship.

3.5. Influence of other structural features upon XynA thermostability

As described above, eleven mutants were obtained for this study and revealed interesting characteristics in relation to the changes in the stability profile and the catalytic performance of XynA.

The change of the first cysteine in the C255–C261 disulfide bond (Fig. 4), which is conserved in the majority of the F/10 family xylanases [22], by a Gly residue, resulted in reduced activity and thermal tolerance, with almost complete denaturation after 1 h at 60 °C, confirming that this interaction is crucial for proper protein folding, stability, and activity [49]. Not all three His residues exercise a significant role in enzymatic activity at high temperatures – onlyH209N, which presented the highest thermostability values in this study (Table 3). The higher number of weak interactions and structural artifacts (short helices and salt bridges) in relation to the native form of XynA might also be related to this increase in thermostability, as suggested by literature [18,23,50–53]. Short helices contribute to the increase in thermostability because they decrease the connecting loops between the elements of secondary structure, making it more regular and rigid and less flexible, thus favoring thermal stability increase [18,50].

Furthermore, of the other six mutants which were developed with a higher number of acidic and basic amino acids than the native form, only N257D presented an increase in the number of salt bridges and short helices, while Q158R had the number of short helices increased, in both cases improving thermostability. The salt bridges are formed by oppositely charged groups, with a distance of up to 4 Å. When located in the kernel, these interactions may contribute with a 3–5 kcal mol^{-1} increase in its stability, whereas these same interactions in the surfaces can only marginally contribute to stabilization [54]. Therefore, a high concentration of salt bridges, particularly networks stitches, in the structure of a protein, makes it more resistant to local deformation, melting or unfolding at high temperatures. In this sense, salt bridges have been observed as beneficial for protein stability and folding [55].

4. Conclusions

The *endo*-1,4-β-xylanase from *Thermoascus aurantiacus* had its thermostability successfully improved by SDM. Based on rational design, eleven mutants were proposed, three of which (Q158R, H209N and N257D)exhibited the best performance in thermosta-

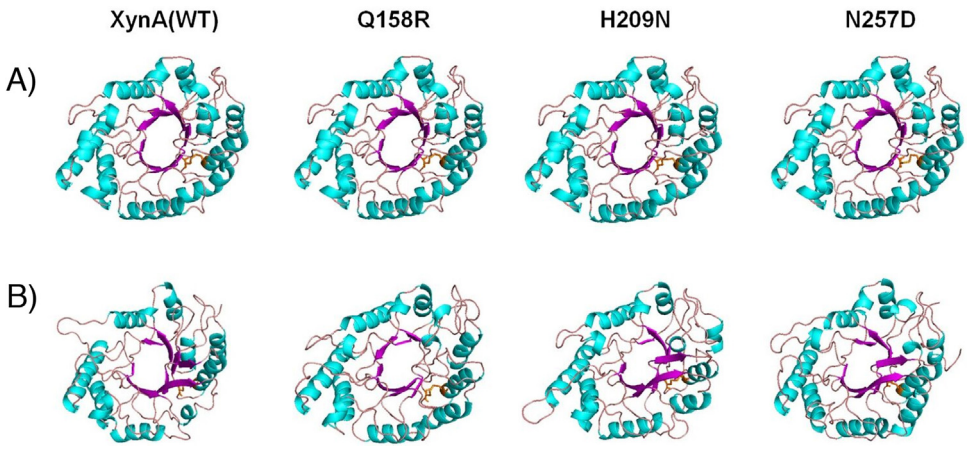

Fig. 4. Models of XynA (WT) and its mutants. (A), Before the simulation. (B), After the simulation of 50 ns in water with NaCl (100 mM) at 338 K. The helices are in cyan, the sheet in purple and the loops in wheat. The disulphide bridge between C255 and C261 is in orange.

bility assays. The results of CD indicate that the enzymes were correctly folded. T*m* values proved they are thermophilic enzymes, with the mutant H209N presenting the highest T*m*. This mutant had an increase of four salt interactions and three short helices and presented a positive charge in the substrate binding active site region. MDS data added important information about the thermostability of the xylanase mutants and WT, revealing a positive correlation of thermostability to the content of positive charges in the enzymatic core. The best mutants generated, as well as XynA (WT), show high biotechnological potential and can be good candidates for future approaches using directed evolution to obtain other mutants with even greater thermostability, as well as other interesting proprieties for industry.

Acknowledgements

This work was funded by São Paulo Research Foundation (FAPESP), with the external scholarship abroad, 2014/04272-8, and the follwing FAPESP grants in Brazil 2011-22461-4, 02/08355-8, 2010/12624-0, 2014/02080-4, and also by CNPq grants 487552/2012-1 and 306044/2014-5. The authors would also like to thank V.B.P. Leite's cluster (FAPESP grant 2011/17658-3) for the computational resources and CNPEM – LAM for the acquisition of the biophysical data.

Appendix A. Supplementary data

Supplementary data associated with this article can be found, in the online version, at http://dx.doi.org/10.1016/j.ijbiomac.2016.08.056.

References

[1] L. Viikari, A. Kantelinen, J. Buchert, J. Puls, Enzymatic accessibility of xylans in lignocellulosic materials, Appl. Microbiol. Biotechnol. 41 (1994) 124–129, http://dx.doi.org/10.1007/BF00166093.
[2] M.P. Coughlan, G.P. Hazlewood, Beta-1 4-D-xylan-degrading enzyme systems: biochemistry, molecular biology and applications, Biotechnol. Appl. Biochem. 17 (Pt. 3) (1993) 259–289.
[3] H. Hori, A.D. Elbein, The biosynthesis of plant cell wall polysaccharides, in: T. Higuchi (Ed.), Biosynth. Biodegrad. Wood Components, Academic Press Inc., 1985, pp. 109–135.
[4] C. Zhou, J. Bai, S. Deng, J. Wang, J. Zhu, M. Wu, et al., Cloning of a xylanase gene from Aspergillus usamii and its expression in Escherichia coli, Bioresour. Technol. 99 (2008) 831–838, http://dx.doi.org/10.1016/j.biortech.2007.01.035.
[5] M.L. Polizeli, A.C. Rizzatti, R. Monti, H.F. Terenzi, J.A. Jorge, D.S. Amorim, Xylanases from fungi: properties and industrial applications, Appl. Microbiol. Biotechnol. 67 (2005) 577–591, http://dx.doi.org/10.1007/s00253-005-1904-7.
[6] H. Liu, J.H. Naismith, An efficient one-step site-directed deletion, insertion, single and multiple-site plasmid mutagenesis protocol, BMC Biotechnol. 8 (2008) 91, http://dx.doi.org/10.1186/1472-6750-8-91.
[7] Q.K. Beg, M. Kapoor, L. Mahajan, G.S. Hoondal, Microbial xylanases and their industrial applications: a review, Appl. Microbiol. Biotechnol. 56 (2001) 326–338, http://dx.doi.org/10.1007/s002530100704.
[8] S. Wu, B. Liu, X. Zhang, Characterization of a recombinant thermostable xylanase from deep-sea thermophilic Geobacillus sp. MT-1 in East Pacific, Appl. Microbiol. Biotechnol. 72 (2006) 1210–1216, http://dx.doi.org/10.1007/s00253-006-0416-4.
[9] N. Kulkarni, A. Shendye, M. Rao, Molecular and biotechnological aspects of xylanases, FEMS Microbiol. Rev. 23 (1999) 411–456, http://dx.doi.org/10.1016/S0168-6445(99)00006-6.
[10] D.G. Olson, J.E. McBride, A.J. Shaw, L.R. Lynd, Recent progress in consolidated bioprocessing, Curr. Opin. Biotechnol. 23 (2012) 396–405, http://dx.doi.org/10.1016/j.copbio.2011.11.026.
[11] R. Prade, Xylanases: from biology to biotechnology, Biotechnol. Genet. Eng. Rev. (1996), http://dx.doi.org/10.1080/02648725.1996.10647925 (accessed 20.03.16) http://www. tandfonline. com//pdf/.
[12] O. Turunen, K. Etuaho, F. Fenel, J. Vehmaanperä, X. Wu, J. Rouvinen, et al., A combination of weakly stabilizing mutations with a disulfide bridge in the α-helix region of Trichoderma reesei endo-1 4-β-xylanase II increases the thermal stability through synergism, J. Biotechnol. 88 (2001) 37–46, http://dx.doi.org/10.1016/S0168-1656(01)00253-X.
[13] T. Beliën, I.J. Joye, J.A. Delcour, C.M. Courtin, Computational design-based molecular engineering of the glycosyl hydrolase family 11 B. subtilis XynA endoxylanase improves its acid stability, Protein Eng. Des. Sel. 22 (2009) 587–596, http://dx.doi.org/10.1093/protein/gzp024.
[14] J. Georis, F. de Lemos Esteves, J. Lamotte-Brasseur, V. Bougnet, B. Devreese, F. Giannotta, et al., An additional aromatic interaction improves the thermostability and thermophilicity of a mesophilic family 11 xylanase: structural basis and molecular study, Protein Sci. 9 (2000) 466–475, http://dx.doi.org/10.1110/ps.9.3.466.
[15] D.Z. Ayadi, A. Hmida Sayari, H. Ben Hlima, S. Ben Mabrouk, M. Mezghani, S. Bejar, Improvement of Trichoderma reesei xylanase II thermal stability by serine to threonine surface mutations, Int. J. Biol. Macromol. 72 (2015) 163–170, http://dx.doi.org/10.1016/j.ijbiomac.2014.08.014.
[16] R. Ruller, L. Deliberto, T.L. Ferreira, R.J. Ward, Thermostable variants of the recombinant xylanase A from Bacillus subtilis produced by directed evolution show reduced heat capacity changes, Proteins 70 (2008) 1280–1293, http://dx.doi.org/10.1002/prot.21617.
[17] R. Ruller, J. Alponti, L.A. Deliberto, L.M. Zanphorlin, C.B. Machado, R.J. Ward, Concommitant adaptation of a GH11 xylanase by directed evolution to create an alkali-tolerant/thermophilic enzyme, Protein Eng. Des. Sel. 27 (2014) 255–262, http://dx.doi.org/10.1093/protein/gzu027.
[18] R. Natesh, P. Bhanumoorthy, P.J. Vithayathil, K. Sekar, S. Ramakumar, M.A. Viswamitra, Crystal structure at 1.8 A resolution and proposed amino acid sequence of a thermostable xylanase from Thermoascus aurantiacus, J. Mol. Biol. 288 (1999) 999–1012, http://dx.doi.org/10.1006/jmbi.1999.2727.
[19] L.U.L. Tan, P. Mayers, J.N. Saddler, Purification and characterization of a thermostable xylanase from a thermophilic fungus Thermoascus aurantiacus, Can. J. Microbiol. (1987), http://dx.doi.org/10.1139/m87-120 (accessed 20.03.16) http://www.nrcresearchpress.com//abs/#.Vu6u5OIrLcc.
[20] F.C. [UNESP] Franco, Clonagem E Expressão Heteróloga Do Gene De Uma Xilanase De Thermoascus Aurantiacus Em Pichia Pastoris, Universidade Estadual Paulista (UNESP), 2011.
[21] E.S. Martins, D. Silva, R.S.R. Leite, E. Gomes, Purification and characterization of polygalacturonase produced by thermophilic Thermoascus aurantiacus CBMAI-756 in submerged fermentation, Antonie Van Leeuwenhoek 91 (2007) 291–299, http://dx.doi.org/10.1007/s10482-006-9114-6.

[22] K.M. Khandke, P.J. Vithayathil, S.K. Murthy, Purification of xylanase, β-glucosidase, endocellulase, and exocellulase from a thermophilic fungus, Thermoascus aurantiacus, Arch. Biochem. Biophys. 274 (1989) 491–500, http://dx.doi.org/10.1016/0003-9861(89)90462-1.
[23] M. Sadeghi, H. Naderi-Manesh, M. Zarrabi, B. Ranjbar, Effective factors in thermostability of thermophilic proteins, Biophys. Chem. 119 (2006) 256–270, http://dx.doi.org/10.1016/j.bpc.2005.09.018.
[24] S.C. Gill, P.H. von Hippel, Calculation of protein extinction coefficients from amino acid sequence data, Anal. Biochem. 182 (1989) 319–326, http://dx.doi.org/10.1016/0003-2697(89)90602-7.
[25] U.K. Laemmli, Cleavage of structural proteins during the assembly of the head of bacteriophage T4, Nature 227 (1970) 680–685, http://dx.doi.org/10.1038/227680a0.
[26] G.L. Miller, Use of dinitrosalicylic acid reagent for determination of reducing sugar, Anal. Chem. 31 (1959) 426–428, http://dx.doi.org/10.1021/ac60147a030.
[27] M.J. Bailey, P. Biely, K. Poutanen, Interlaboratory testing of methods for assay of xylanase activity, J. Biotechnol. 23 (1992) 257–270, http://dx.doi.org/10.1016/0168-1656(92)90074-J.
[28] A. Bhalla, K.M. Bischoff, N. Uppugundla, V. Balan, R.K. Sani, Novel thermostable endo-xylanase cloned and expressed from bacterium Geobacillus sp. WSUCF1, Bioresour. Technol. 165 (2014) 314–318, http://dx.doi.org/10.1016/j.biortech.2014.03.112.
[29] A. Šali, T.L. Blundell, Comparative protein modelling by satisfaction of spatial restraints, J. Mol. Biol. 234 (1993) 779–815, http://dx.doi.org/10.1006/jmbi.1993.1626.
[30] H.J.C. Berendsen, J.P.M. Postma, W.F. van Gunsteren, a DiNola, J.R. Haak, Molecular dynamics with coupling to an external bath, J. Chem. Phys. 81 (1984) 3684–3690, http://dx.doi.org/10.1063/1.448118.
[31] S. Pronk, S. Páll, R. Schulz, P. Larsson, P. Bjelkmar, R. Apostolov, et al., GROMACS 4.5: a high-throughput and highly parallel open source molecular simulation toolkit, Bioinformatics 29 (2013) 845–854, http://dx.doi.org/10.1093/bioinformatics/btt055.
[32] C. Oostenbrink, A. Villa, A.E. Mark, W.F. van Gunsteren, A biomolecular force field based on the free enthalpy of hydration and solvation: the GROMOS force-field parameter sets 53A5 and 53A6, J. Comput. Chem. 25 (2004) 1656–1676, http://dx.doi.org/10.1002/jcc.20090.
[33] H.J.C. Berendsen, J.P.M. Postma, W.F. van Gunsteren, J. Herman, Intermolecular Forces, Springer, Netherlands, Dordrecht, 1981, http://dx.doi.org/10.1007/978-94-015-7658-1.
[34] G. Bussi, D. Donadio, M. Parrinello, Canonical sampling through velocity rescaling, J. Chem. Phys. 126 (2007) 1–7, http://dx.doi.org/10.1063/1.2408420.
[35] H.J.C. Berendsen, D. van der Spoel, R. van Drunen, GROMACS: a message-passing parallel molecular dynamics implementation, Comput. Phys. Commun. 91 (1995) 43–56, http://dx.doi.org/10.1016/0010-4655(95)00042-E.
[36] U. Essmann, L. Perera, M.L. Berkowitz, T. Darden, H. Lee, L.G. Pedersen, A smooth particle mesh Ewald method, J. Chem. Phys. 103 (1995) 8577–8593, http://dx.doi.org/10.1063/1.470117.
[37] R.A. Laskowski, M.W. MacArthur, D.S. Moss, J.M. Thornton, PROCHECK: a program to check the stereochemical quality of protein structures, J. Appl. Crystallogr. 26 (1993) 283–291, http://dx.doi.org/10.1107/S0021889892009944.
[38] L. Schrödinger, The PyMOL Molecular Graphics System, 2010.
[39] S. Costantini, G. Colonna, A. Facchiano, ESBRI: A Web Server for Evaluating Salt Bridges in Proteins, Bioinformation, 2008 (accessed 31.03.16) https://www.researchgate.net/profile/Giovanni_Colonna/publication/26552830_ESBRI_A_web_server_for_evaluating_salt_bridges_in_proteins/links/02bfe5117acc4a6cb0000000.pdf.
[40] A. Lejeune, M. Vanhove, J. Lamotte-Brasseur, R.H. Pain, J.-M. Frère, A. Matagne, Quantitative analysis of the stabilization by substrate of Staphylococcus aureus PC1 β-lactamase, Chem. Biol. 8 (2001) 831–842, http://dx.doi.org/10.1016/S1074-5521(01)00053-9.
[41] K.L. Shaw, G.R. Grimsley, G.I. Yakovlev, A.A. Makarov, C.N. Pace, The effect of net charge on the solubility, activity, and stability of ribonuclease Sa, Protein Sci. 10 (2001) 1206–1215, http://dx.doi.org/10.1110/ps.440101.
[42] D. Nath, M. Rao, pH dependent conformational and structural changes of xylanase from an alkalophilic thermophilic Bacillus sp (NCIM 59), Enzyme Microb. Technol. 28 (2001) 397–403, http://dx.doi.org/10.1016/S0141-0229(00)00359-8.
[43] H. Umemoto, Ihsanawati, M. Inami, R. Yatsunami, T. Fukui, T. Kumasaka, et al., Improvement of Alkaliphily of Bacillus Alkaline Xylanase by Introducing Amino Acid Substitutions Both on Catalytic Cleft and Protein Surface, 2014 http://dx.doi.org/10.1271/bbb.80869.
[44] Y. Wang, S. Feng, T. Zhan, Z. Huang, G. Wu, Z. Liu, Improving catalytic efficiency of endo-β-1 4-xylanase from Geobacillus stearothermophilus by directed evolution and H179 saturation mutagenesis, J. Biotechnol. 168 (2013) 341–347, http://dx.doi.org/10.1016/j.jbiotec.2013.09.014.
[45] Y. Wang, Z. Fu, H. Huang, H. Zhang, B. Yao, H. Xiong, et al., Improved thermal performance of Thermomyces lanuginosus GH11 xylanase by engineering of an N-terminal disulfide bridge, Bioresour. Technol. 112 (2012) 275–279, http://dx.doi.org/10.1016/j.biortech.2012.02.092.
[46] J. Jänis, J. Rouvinen, P. Vainiotalo, O. Turunen, V.L. Shnyrov, Irreversible thermal denaturation of Trichoderma reesei endo-1 4-β-xylanase II and its three disulfide mutants characterized by differential scanning calorimetry, Int. J. Biol. Macromol. 42 (2008) 75–80, http://dx.doi.org/10.1016/j.ijbiomac.2007.09.012.
[47] A. Akasako, M. Haruki, M. Oobatake, S. Kanaya, Conformational stabilities of Escherichia coli RNase HI variants with a series of amino acid substitutions at a cavity within the hydrophobic core, J. Biol. Chem. 272 (1997) 18686–18693, http://dx.doi.org/10.1074/jbc.272.30.18686.
[48] D.N. Woolfson, Core-directed protein design, Curr. Opin. Struct. Biol. 11 (2001) 464–471, http://dx.doi.org/10.1016/S0959-440X(00)00234-7.
[49] B. Kong, G.L. Guo, Soluble expression of disulfide bond containing proteins FGF15 and FGF19 in the cytoplasm of *Escherichia coli*, PLoS One 9 (2014) e85890 http://dx.doi.org/10.1371%2Fjournal.pone.0085890.
[50] G. Auerbach, R. Ostendorp, L. Prade, I. Korndorfer, T. Dams, R. Huber, et al., Lactate dehydrogenase from the hyperthermophilic bacterium thermotoga maritima: the crystal structure at 2.1 A resolution reveals strategies for intrinsic protein stabilization, Structure 6 (1998) 769–781.
[51] A.H. Elcock, The stability of salt bridges at high temperatures: implications for hyperthermophilic proteins, J. Mol. Biol. 284 (1998) 489–502, http://dx.doi.org/10.1006/jmbi.1998.2159.
[52] R.B. Freedman, Proteins: structures and molecular properties, Trends Biochem. Sci. 10 (1985) 82, http://dx.doi.org/10.1016/0968-0004(85)90239-7.
[53] L. Ellegaard-Jensen, J. Aamand, B.B. Kragelund, A.H. Johnsen, S. Rosendahl, Strains of the soil fungus Mortierella show different degradation potentials for the phenylurea herbicide diuron, Biodegradation 24 (2013) 765–774, http://dx.doi.org/10.1007/s10532-013-9624-7.
[54] D.E. Anderson, W.J. Becktel, F.W. Dahlquist, pH-induced denaturation of proteins: a single salt bridge contributes 3–5 kcal/mol to the free energy of folding of T4 lysozyme, Biochemistry 29 (1990) 2403–2408.
[55] S. Kumar, R. Nussinov, How do thermophilic proteins deal with heat? Cell Mol. Life Sci. 58 (2001) 1216–1233, http://dx.doi.org/10.1007/PL00000935.